Raman scattering and thermogravimetric analysis of iodine-doped multiwall carbon nanotubes

Weiya Zhou,[a] Sishen Xie, Lianfeng Sun, Dongsheng Tang, Yubao Li, Zuqin Liu, Lijie Ci, Xiaoping Zou, and Gang Wang
Institute of Physics and Center for Condensed Matter Physics, Chinese Academy of Sciences, P.O. Box 603, Beijing 100080, People's Republic of China

Pingheng Tan
National Laboratory for Superlattice and Microstructures, P.O. Box 912, Beijing 100083, People's Republic of China

Xiaoli Dong, Bo Xu, and Boru Zhao
National Laboratory of Superconductivity, Institute of Physics and Center for Condensed Matter Physics, Chinese Academy of Sciences, Beijing 100080, People's Republic of China

(Received 19 July 2001; accepted for publication 8 February 2002)

Iodine-doped multiwall carbon nanotubes (I-MWNTs) were characterized by means of Raman scattering and thermogravimetric analysis. The results show that multiwall carbon nanotubes (MWNTs) can be effectively doped by iodine and exchange electrons with iodine. Iodine atoms form charged polyiodide chains inside tubes of different inner diameter, which is similar to the iodine-doped single-wall carbon nanotubes (I-SWNTs), but can not intercalate into the graphene walls of MWNTs. The Raman scattering behavior of I-MWNTs exhibits some differences from that of I-SWNTs and the low-dimensional conductive hydrocarbon-iodine complex "perylene$\cdot I_{2.92}$." © *2002 American Institute of Physics.* [DOI: 10.1063/1.1468269]

Carbon nanotubes and graphite are polymorph solids. They can be doped by guest species. In many instances, the doping leads to charge transfer between the guest species (a dopant atom or molecular) and the host. Both graphite[1] and single-wall carbon nanotube (SWNT)[2–5] have been shown to be amphoteric in character, that is, they can exchange electrons with a dopant to form a corresponding positively or negatively charged counterion. However, it is of interest to note that iodine can dope effectively into SWNTs,[5–7] whereas it can not intercalate into graphite[1] because of its large van der Waals diameter (0.396 nm)[8] and interatomic spacing (0.27 nm) incompatible with any spacing of the basal plane in graphite.[9,10] Raman scattering showed charged polyiodide ions to be distributed throughout the doped SWNTs bundles.[6] The images of atomic resolution *Z*-contrast scanning transmission electron microscopy[7] were taken for the doped nanotubes which protruded beyond the ends of the iodine-doped bundles, revealing the incorporation of iodine atoms in the form of helical chains inside the SWNT. Density functional calculations and topological considerations confirmed that charge transfer actually occurs between iodine and the nanotube wall in the case of linear I_5^- and I_3^- intercalated molecules.

To date, a few studies on the iodine-doped carbon nanotubes have mainly focused on the iodine-doped SWNTs (I-SWNTs),[2–7] but little is known about the iodine-doped MWNTs (I-MWNTs). In this letter, we characterize the I-MWNTs by thermogravimetric analysis (TGA) and Raman scattering spectroscopy. Some common features and dissimilarities between I-MWNTs and I-SWNTs were observed.

The MWNTs used in this study were synthesized by the arc discharge method[11] and subsequently oxidized in air at 700 °C for about 1 h to open ended nanotubes. Scanning electron microscopy and transmission electron microscopy (TEM) images showed that the MWNTs were purely multiwalled, dispersive, end open, and randomly oriented. On an average, the graphene walls of the MWNTs consist of 15 layers and the inner diameters of the MWNTs range from 0.5 to 7.5 nm with a mean of 3.66 nm. Intercalation was carried out by immersing the MWNTs into molten iodine[6] in an evacuated quartz tube at a temperature $T=140\,^{\circ}\mathrm{C}$ ordinarily for one week. In order to remove excess physisorbed iodine, the samples were heat treated as follows. The end of the quartz tube containing the doped MWNTs was heated to about 70 °C for 5–6 h, while the other end was submerged in liquid nitrogen to collect the vaporized iodine.

TGA experiments were carried out using a Rheometric Scientific ThermoGravimetric Analyzer TGA MK II. The sample was heated from 16 °C to 700 °C at a rate of 2 °C/min in ultrapure Ar gas flow (8 ml/min) while monitoring the weight loss. Raman scattering spectra were recorded by the Dilor Super Labram with a typical resolution of 1 cm^{-1}. All the spectra reported here were measured in backscattering geometry using 514.5 and 632.8 nm laser excitation wavelengths. Typically, a low laser power of 20 $\mathrm{kW/cm}^2$ was used to avoid sample heating, and a spatial resolution of less than 2 μm was achieved using a microscope with a 100× objective lens.

Figure 1 shows TGA curves of pristine (a) and *I*-doped (b) MWNT samples. Two noticeable weight losses could be observed for I-MWNTs: the first weight loss commenced at room temperature and ended at $T\sim200\,^{\circ}\mathrm{C}$, the second occurred at $T\sim420\,^{\circ}\mathrm{C}$ and did not finish up to 700 °C. By comparison with the TGA curve of purified MWNTs (curve a in Fig. 1) where only one weight loss starting at $T\sim530\,^{\circ}\mathrm{C}$ was observed, it is evident that the first loss shown in curve

[a]Electronic mail: wyzhou@aphy.iphy.ac.cn

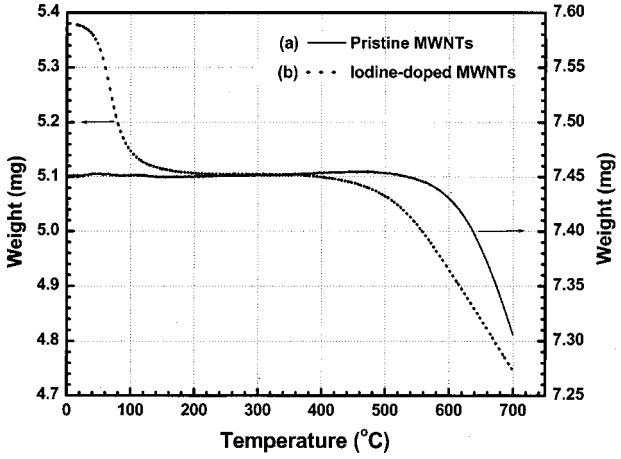

FIG. 1. TGA curves of pristine (a) and I-doped (b) MWNT samples.

b in Fig. 1 is corresponding to the loss of the intercalated iodine in MWNTs and its commencing temperature is different from that of I-SWNTs (at $T\sim100\,^{\circ}\mathrm{C}$).[6] The commencing temperature of the second weight loss is about 100 °C lower than that of the purified pristine MWNTs. The weight loss in MWNTs as well as in I-MWNTs at a higher temperature is likely to be related to the carbonization process.[12]

In Fig. 2 are presented Raman scattering spectra ($T=300$ K and 514.5 nm laser excitation) of pristine (a) and I-MWNT samples [fresh (b), kept in desiccator for one year (c) and nearly iodine free after TGA measurement (d), removing iodine by heating the sample for 5 h at about 673 K under a vacuum of 10^{-4} Pa (e)]. For pristine MWNTs, several radial breathing modes are located in the range of 110–270 cm^{-1} corresponding to the inner diagrams of MWNTs in the range of 0.9–2 nm according to theoretical predictions.[13] Experimental observation of the radial breathing modes of MWNTs was also reported by Ando *et al.*[14] However, for a fresh iodine-doped sample [Fig. 2(b)], two new bands not associated with MWNTs are observed distinctly at $\omega_0=\sim170s$ ($s=$strong) and $\sim111m$ ($m=$middle) cm^{-1} in the low frequency region, and their harmonic series ($2\omega_0,\ldots$) also appear despite their weak intensities. We did not observe any Raman peaks around 215 cm^{-1} (Ref. 15) which would be expected if neutral or dissociative molecular iodine $(I_2)^0$ were present in the samples. This indicates that no excessive iodine exists in the sample after removing excess physisorbed iodine effectively although iodine can ooze slowly out of the as-prepared iodine-intercalated MWNTs at room temperature. In Fig. 2(c), a new peak at $137w$ cm^{-1} ($w=$weak), which appears in Raman spectra of moderately I-SWNTs,[6] can be observed for a sample kept in a desiccator at room temperature for one year. It is very interesting that both the intensity and the frequency of these three new bands for I-MWNTs remarkably mimic those for I-SWNTs.[6] By comparison of the Raman spectra of I-MWNTs with that of I-SWNTs and hydrocarbon–iodine complex "perylene$\cdot I_{2.92}$,"[15] they are very similar to each other regarding the peak position and the relative intensities of the peaks in the low frequency region. It is reasonable to attribute the strong 170 and middle 111 cm^{-1} peaks and their overtone progressions to resonant Raman scattering from charged $(I_5)^{-1}$ and

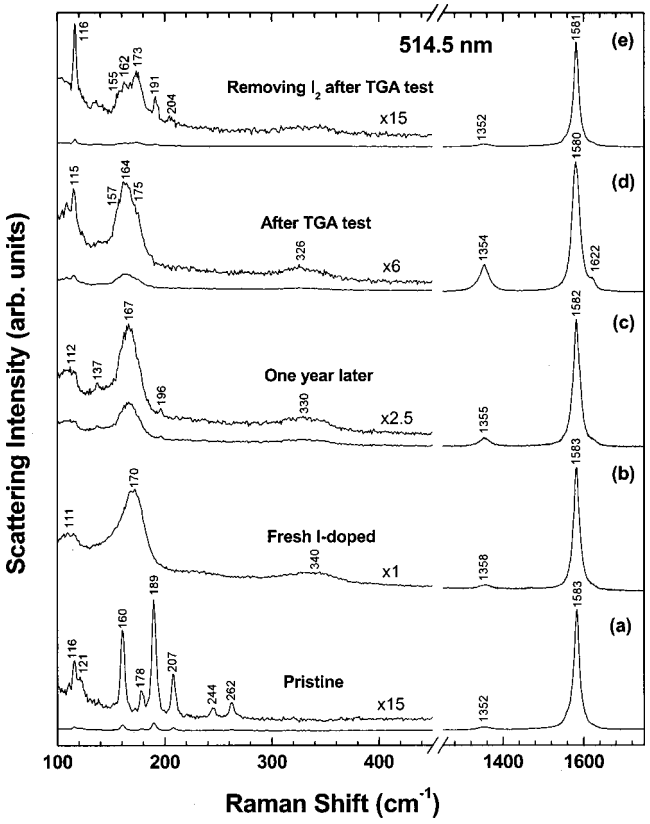

FIG. 2. Raman spectra ($T=300$ K and 514.5 nm laser excitation) of pristine (a) and I-doped MWNT samples [fresh (b), kept in and desiccator for one year (c), almost removed I_2 after TGA measurement (d), and removing iodine by heating the sample for 5 h at about 673 K under a vacuum of 10^{-4} Pa (e)].

$(I_3)^{-1}$ linear chain complexes, respectively, and to assign the weak 137 cm^{-1} as that from $(I_3)^{-1}$ chain.

The intensity of the strongest peak (denoted as I_I) in the low frequency region is close to that of G band (denoted as I_G) around 1583 cm^{-1} assigned to a tangential C-atom displacement mode, i.e., $I_I/I_G\approx1$, for fresh I-MWNTs. As outdiffusing of iodine occurs ceaselessly at room temperature, the intensity at $\omega_0=\sim170s$ cm^{-1} decreases, $I_I/I_G<1$. After removing iodine designedly by heating, $I_I/I_G\ll1$ [Fig. 2(e)], and I_I is comparable to the intensities of the breathing modes of the undoped MWNTs, which means that most of iodine in the I-MWNTs has been deintercalated. When the time and temperature of heat treatment increase, neither $(I_5)^{-1}$ band nor $(I_3)^{-1}$ bands was observed at low frequency range, indicating a complete removal of iodine. As most of the intercalated iodine was removed by heating the sample, several sharp peaks appeared beside or overriding on the broad bands at 170 and 111 cm^{-1} [Fig. 2(e)]. These new sharp peaks can be assigned as the breathing mode peaks corresponding to the undoped MWNTs. This implies that iodine intercalation of MWNTs is reversible.

As indicated in Fig. 2(d), most of the intercalated iodine was removed after a TGA test. We can estimate the composition of a sample by the first weight loss in the TGA curve. An average composition for a fresh I-MWNTs is close to IC_{200}—this ratio of I:C is far lower than that of IC_{12} for I-SWNTs.[6] First-principle calculation showed that in a simple (10, 10) SWNT of 1.36 nm in diameter, iodine can exist stably in forms of helical chains with a period of 12.5,

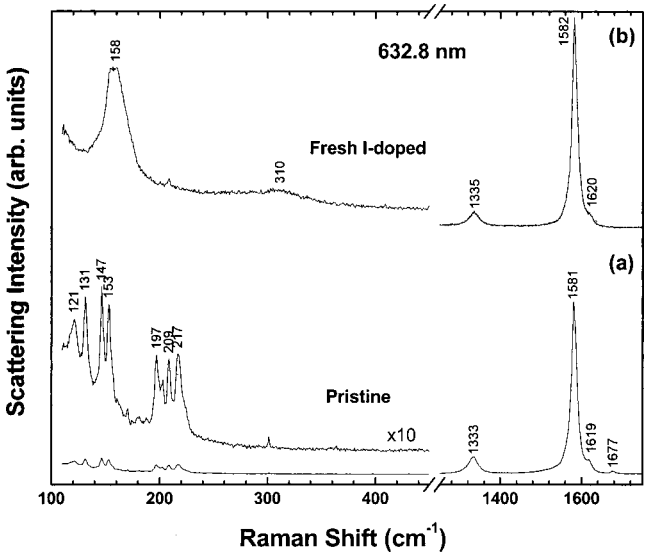

FIG. 3. Raman spectra of pristine MWNTs (a) and I-MWNTs (b) taken with 632.8 nm excitation ($T=300$ K).

5, or 1.5 nm, which is consistent with the *Z*-contrast images of I-SWNTs.[7] The calculation reveals the saturation doping levels of IC_{15} and IC_8 in the (10, 10) SWNTs with the iodine strands of 1.5 and 5 nm helical periods, respectively. For a SWNT with a larger diameter, there would be sufficient room for more chains. Provided the incorporated iodine exists, in forms of helical chains, exclusively inside the innermost tube of the MWNTs with an average thickness of 15 layers and an average diameter of 3.66 nm, the estimated composition IC_{200} can be scaled to a composition of IC'_6, where C' counts only the carbon on the innermost tube wall. In other words, IC_6 would correspond to a composition of I-SWNTs with a diameter of 3.66 nm. Therefore, from the TGA data of the I-MWNTs, one may infer that iodine or iodine chains can not be incorporated into the graphene multishells of the MWNTs, which could be attributed to the fact that the spacing between graphene sheets of MWNTs is almost the same as in graphite and can not accommodate larger iodine or iodine chains.

The Raman scattering data on the same samples of pristine MWNTs, iodine (omitted here) and I-MWNTs were also collected with different (514.5 and 632.8 nm) laser excitation ($T=300$ K). The Raman spectra of I_2 and perylene$\cdot I_{2.92}$[15] were essentially independent of exciting wavelength of 632.8 and 514.5 nm. However, we found that the peak frequencies for I-MWNTs as well as for pristine MWNTs varied with laser excitation frequency, though *G* band was not influenced noticeably under these two excitation frequencies. For example, the position of the strong band (I_5^-) peak is at $\sim$170 cm^{-1} with 514.5 nm excitation [Fig. 2(b)] and shifts to $\sim$158 cm^{-1} with 632.8 nm excitation [Fig. 3(b)]. The middle strong band (I_3^-) peak exists evidently at 111 cm^{-1} in Fig. 2(b) but is not observed in Fig. 3(b). This peak may have downshifted below our lower frequency limit ($\sim$110 cm^{-1}). The dramatic changes (or shifts) with laser excitation frequency of both the Raman peak intensities and frequencies in low frequency region, for pristine MWNTs in Figs. 2(a) and 3(a) as well as the I-MWNTs in Figs. 2(b) and 3(b), could be attributed to diameter-dependent optical absorption that promotes resonant scattering from particular diameter tubes.[16,17] This result, therefore, reveals further that iodine, in the form of linear I_5^- and I_3^- molecules, intercalates into the innermost tubes of different diameters of the MWNTs.

Due to a transfer of carbon π-electrons to the intercalant, a contraction of the hexagonal rings along the cylindrical wall is expected,[1] which may result in an upshift of the frequencies of the tangential mode for iodine-intercalated carbon nanotubes. The high-frequency Raman triplet of SWNTs was strongly affected by polyiodide chain intercalation. The shift of these modes for I-SWNTs could be as large as 8 cm^{-1}.[6] However, the frequency of the C—C stretching Raman-active *G* mode at 1583 cm^{-1} for purified MWNTs was hardly dependent of iodine intercalation. This observation can be understood by taking into account the fact that multishelled carbon nanotubes contain tubes with different diameters that contribute to the *G* mode in Raman spectrum separately.[16–18] The intensity of the Raman peak can be approximated by the number of bonds. Because the number of bonds is proportional to the tube radius, tubes with the largest radius will dominate the spectrum if the Raman cross section is assumed to be constant for different tube diameters. Since the MWNTs in our present study consist of, on average, 15 layers and the tangential stretching mode around 1582 cm^{-1} is dominated by the outer shells, while iodine ions incorporate exclusively in the innermost tube and the interaction between iodine and the carbon on outer shell is small, it is reasonable that the effect of iodine intercalation on the tangential stretching mode is very small.

This work is supported by NSFC and ''973'' National Key Basic Research Project.

[1] M. S. Dresselhaus and G. Dresselhaus, Adv. Phys. **30**, 139 (1981).
[2] R. S. Lee, H. J. Kim, J. E. Fischer, A. Thess, and R. E. Smalley, Nature (London) **388**, 255 (1997).
[3] A. M. Rao, P. C. Eklund, S. Bandow, A. Thess, and R. E. Smalley, Nature (London) **388**, 257 (1997).
[4] A. M. Rao, S. Bandow, E. Richter, and P. C. Eklund, Thin Solid Films **331**, 141 (1998).
[5] M. S. Dresselhaus and P. C. Eklund, Adv. Phys. **49**, 705 (2000).
[6] L. Grigorian, K. A. Williams, S. Fang, G. U. Sumanasekera, A. L. Loper, E. C. Dickey, S. J. Pennycook, and P. C. Eklund, Phys. Rev. Lett. **80**, 5560 (1998).
[7] X. Fan, E. C. Dickey, P. C. Eklund, K. A. Williams, L. Grigorian, R. Buczko, S. T. Pantelides, and S. J. Pennycook, Phys. Rev. Lett. **84**, 4621 (2000).
[8] R. H. Baughman, S. L. Hsu, L. R. Anderson, G. P. Pez, and A. J. Signorelli, in *Molecular Metals, NATO Conference Series, Series VI: Materials Science Volume 1*, edited by W. E. Hatfield (Plenum, New York, 1979), p. 187.
[9] S. Nakashima, M. Norimoto, H. Harima, Y. Hamanaka, L. S. Grigoryan, and M. Tokumoto, Chem. Phys. Lett. **268**, 359 (1997).
[10] H. Werner, M. Wesemann, and R. Schlogl, Europhys. Lett. **20**, 107 (1992).
[11] B. H. Chang, S. S. Xie, W. Y. Zhou, L. X. Qian, Z. W. Pan, J. M. Mao, and W. Z. Li, J. Mater. Sci. Lett. **17**, 1015 (1998).
[12] R. Saito, G. Dresselhaus, and M. S. Dresselhaus, in *Physical Properties of Carbon Nanotubes* (Imperial College Press, London, 1998), p. 87.
[13] V. N. Popov, V. E. van Doren, and M. Balkanski, Phys. Rev. B **59**, 8355 (1999).
[14] Y. Ando, X. Zhao, and H. Shimoyama, Carbon **39**, 569 (2001).
[15] R. C. Teitelbaum, S. L. Ruby, and T. J. Marks, J. Am. Chem. Soc. **101**, 7568 (1979).
[16] E. Richter and K. R. Subbaswamy, Phys. Rev. Lett. **79**, 2738 (1997).
[17] P. H. Tan, Y. Tang, Y. M. Deng, F. Li, L. Wei, and H. M. Cheng, Appl. Phys. Lett. **75**, 1524 (1999).
[18] W. S. Bacsa, D. Ugarte, A. Châtelain, and W. A. de Heer, Phys. Rev. B **50**, 15473 (1994).